Geophysical assessment for gold mineralization potential over the southern part of Kebbi State using aeromagnetic data

Abdulrahaman Idris Augie[1], Kazeem Adeyinka Salako[2],
Adewuyi Abdulwaheed Rafiu[3], Mufutau Owolabi Jimoh[4]

[1] Federal University Birnin Kebbi, Department of Applied Geophysics, Nigeria,
e-mail: ai.augie@fubk.edu.ng (corresponding author), ORCID ID: 0000-0001-8554-8531
[2] Federal University of Technology Minna, Department of Geophysics, Nigeria, ORCID ID: 0000-0003-4016-4811
[3] Federal University of Technology Minna, Department of Geophysics, Nigeria, ORCID ID: 0000-0003-2434-4919
[4] Federal University of Technology Minna, Department of Geology, Nigeria

Abstract: The magnetic signatures over the southern part of Kebbi State and its environs were analyzed together with the geological settings of the area to delineate the structures that may host gold mineralization. The aeromagnetic data used was the survey carried out by Fugro airborne surveys between 2005 and 2010 on behalf of the Federal Government of Nigeria. The reduction to equator (RTE), first and second vertical derivatives (FVD and SVD), Centre for Exploration Targeting (CET), analytic signal (AS), source parameter imaging (SPI) and tilt derivative (TDR) techniques were applied to the magnetic data covering the area. The results of the AS technique revealed that the study area is characterized with high amplitudes of magnetic anomalies (above 0.048 nT/m) and these could be of ferromagnetic minerals such as gold. The FVD, SVD, CET and TDR techniques also helped in delineating the lineaments (such as faults, fractures or shears zones) believed to be associated with alteration zones which play an important role in determining gold mineralized zones. The direction of the orientation of these features/lineaments trended in the NE-SW direction. The faults, fractures or shears zones delineated represent veins of possible mineralization. The depth of occurrence to the causative bodies using SPI algorithms was found to be below 137 m. Structures delineated within the area, when compared with the geological setting of the area, correspond to: quartz-mica schist, granite, biotite, gneiss, diorite, medium coarse-grained and biotite hornblende granite. Results from these techniques revealed alteration zones that may host gold. These regions correspond to the following areas: SE parts of Yauri and Shanga, Fakai, Ngaski, Zuru, Magama, Rijau, and the eastern part of Wasagu/Danko and Bukkuyum.

Keywords: gold mineralization, Yauri-Zuru schist belt, Centre for Exploration Targeting (CET), first vertical derivatives (FVD), second vertical derivatives (SVD), source parameter imaging (SPI), tilt derivative (TDR)

INTRODUCTION

Nigeria is richly endowed with abundant solid minerals, particularly gold, and which are widely distributed across the country. Mining in Nigeria, and especially of gold, has been viewed as a key driver for economic growth and the development of sustainable social and economic wellbeing (Olalekan et al. 2016, Augie et al. 2021a). Gold deposits in Nigeria are mostly found in quartz veins

as visible gold and also as inclusions in some ore minerals within several metasedimentary and meta-igneous rocks across the diverse supracrustal rocks of the schist belts (Ramadan & Abduel-Fattah 2010, Sani et al. 2019, Augie & Sani 2020, Augie et al. 2021b). Most mineralized zones are structurally controlled and spatially associated with shear zones and hydrothermal veins formed in response to the regional stress field (Kearey et al. 2002, Sani et al. 2017, Augie et al. 2022). These structures may be deep-seated and consequently require geophysical approach to delineate the possible pathways for gold exploration and exploitation (Ejepu et al. 2018).

Structures such as fractures play a very important role in gold mineralization: first as conduits for the mineralization solution and second, as loci of deposition of mineralization fluid (Adetona et al. 2018). Faults and shear zones are potential pathways of fluids (Sani et al. 2019, Tawey et al. 2020) and thus knowledge of the structural architecture of a mineralized area, the distribution and orientation of faults and shear zones, their formation and possible reactivation during the structural evolution and the tectonic conditions are key to understanding the formation, origin and location of mineral deposits (Reeves 2005, Danbatta et al. 2008, Adewumi & Salako 2018, Augie et al. 2021b).

The potential field strategies have a critical influence in subsurface structural mapping and mineral investigation (Evjen 1936, Cardell & Grauch 1985, Roast et al. 1992, Fedi & Florio 2001). The derivative derivative technique was utilized to find the source horizontal boundaries (Evjen 1936). Horizontal gradient amplitude was employed to produce the maximum values over the source edges (Cordell & Grauch 1985). Meanwhile, analytical signal amplitude (AS) filter was used to delineate the lateral boundaries with the highest values of an amplitude signal (Roest et al. 1992). The enhancement of the analytic signal based on higher-order derivatives was used improve the determination of the resolution of the edge detection by Hsu et al. (1996). This prompted the improvement of the high-resolution method to enhance the edges, based on the THDR of a sum of increasing-order vertical gradients by Fedi & Florio (2001).

However, using the previously mentioned potential field techniques can also help determine the information about the horizontal location, profundity and incline of the causative sources associated with minerals (Pham et al. 2019, 2020, 2022). Information on the potential field source edges significantly affects the streamlining of investigation boring activities (Pham 2021). Consequently, the effectiveness of the edge identification strategies requires a precise and sharp outline of the horizontal positions of the bizarre bodies (Pham 2021, Pham et al. 2021).

Mineralization potential has been reported in the area in earlier studies by Ramadan & Abdel Fattah (2010), Bonde et al. (2019), Lawali et al. (2020) and Lawali et al. (2021). These studies used aeromagnetic data for the structural mapping of solid mineral potential zones over the southern part of Kebbi State. The results unanimously led to the delineation of NE-SW trending features such as fractures, faults and veins within which some minerals might found. The study area of this research falls under the low latitude area of the equatorial zones and the reduction to the magnetic equator was not applied by the authors. At low latitudes, a separate amplitude correction is usually required so as to prevent the North-South signal in the data from dominating the results (Holden et al. 2008, Core et al. 2009).

However, efforts have also been made by artisanal miners to trace the minerals, particularly gold at Birnin-Yauri, Yauri, Shanga, Fakai, Sakaba, Zuru and Bagudo which usually occurred as a primary deposit in crystalline basement complex rocks. These artisanal miners use a trial-and-error method of exploitation which makes it nearly impossible to locate the zones harboring these gold minerals. The use of the trial-and-error method has resulted in abandoned pits and trenches which facilitate the pollution of the environment. It has also resulted in low yields due to lack of proper geophysical studies and database of precise coordinates.

This study employed aeromagnetic method with the aim of assessing gold mineralization potential by mapping out the major structural trends that control gold mineralization in the southern part of Kebbi State. Therefore, to locate the potential mineral zones and particularly those of

gold mineralization, the geophysical aeromagnetic method was adopted to delineate near-surface structures within the study area that might be potential host for gold mineralization using: reduction to magnetic equator (RTE), first and second vertical derivatives (FVD and SVD), Centre for Exploration Targeting (CET), analytic signal (AS), source parameter imaging (SPI) and tilt derivative (TDR) techniques with the aid of geological setting of the study area.

The limitations of the FVD, SVD and AS filters are that they sometimes generate false edges in the result-making them less effective in detecting the edge of deep sources or thin sources. Recently, Pham et al. (2019, 2020, 2021, 2022) and Pham (2021) introduced some new methods for detecting lineaments, which show improved performance as edge detection filters. The technique introduced was the improvement of tilt derivative (TDR) developed by Miller & Singh (1994). This used the amplitude of the total horizontal derivative to normalize the vertical derivative. This technique was further improved in order to simultaneously display the edges of the shallow and deep sources as well as wide range of phase-based methods. For this study, TRD, CET, FVD, SVD, AS and SPI filters were applied to RTE to determine the subsurface structures associated with gold mineralization potential and with the help of the magnetic susceptibility for various rock type and the geological setting of the area.

Location and geological settings of the study area

The study area lies within the southern part of Kebbi state and, some part of Zamfara and Niger states between latitudes 10°30′0″N and 12°0′0″N, and longitudes 4°0′0″E and 5°30′0″E. The area covers the following nineteen (19) local government areas (LGAs): Yauri, Zuru, Nngaski, Shanga, Fakai, Danko/Wasagu, Sakaba, Koko Besse, Maiyama, Bagudo and Suru LGAs of Kebbi State including Kebbe, Gummi and Bukkuyum LGAs of Zamfara State and, also Rijau, Agwara, Borgu and Magama LGAs of Niger State (see Fig. 1).

Geologically, the study area falls under the basement complex rocks and some parts of the sedimentary basin. It is comprised of granite, rhyolite, biotite-granite, meta-conglomerate, quartz-mica schist, migmatite, undifferentiated schist including gneiss, sandstones, ironstones and laterites (Fig. 1).

The metasediments in these areas are also comprised of quartzites, schists and phyllites, whereas the older granites consist of granodiorites or diorites. Furthermore, dacites/rhyolites are overlain and intrude the basement gneisses, metasediments and granitic rocks of the southern (Anka-Yauri schist) part of Kebbi (Danbatta 2008). The area also consists of a brittle fault zone which was made up of sub-parallel phyllites, deformed and undeformed quartzites which form part of the mapped Anka transcurrent fault which is known as the possible Pan-African crustal suture (Danbatta 2005).

However, some parts of the study area are underlain by younger sedimentary rocks that comprise mainly sandstones, siltstones, clay shales limestone and laterites (Fig. 1). The sedimentary rocks in the mapped area can be grouped into four major rock types: siltstone (with fine-grained sandstone), medium to coarse-grained sandstone, shale and limestone (Augie et al. 2020, Olugbenga & Augie 2020).

The southern part of the Kebbi of basement complex/schist belt was called Zuru-Yauri schist belt. Danjumma et al. (2019) reported that the Zuru-Yauri schist belt consists of an assemblage of muscovite-biotite banded gneisses, porphyroblastic gneisses, migmatites, schists, quartzites, metavolcanics (amphibolites), quartzites, mica schists, granulites, calc-silicates older granites and minor rocks such as gabbro, andesite, granulites and calcsilicates. The structural elements in the Zuru-Yauri schist belt are the major NNE-SSW to NE-SW trending Birnin-Yauri, Yauri and Ribah dextral faults, a NW-SE trending Gunusinistral fault and a major N-S trending anticlinorium known as the Zuru anticlinorium (Danbatta 2005, Sani et al. 2019). These schists differ lithologically from the other schist belt in north-western Nigeria and it is predominantly composed of quartzites with very subordinate schists and amphibolites (Danbatta 2008, Danjumma et al. 2019).
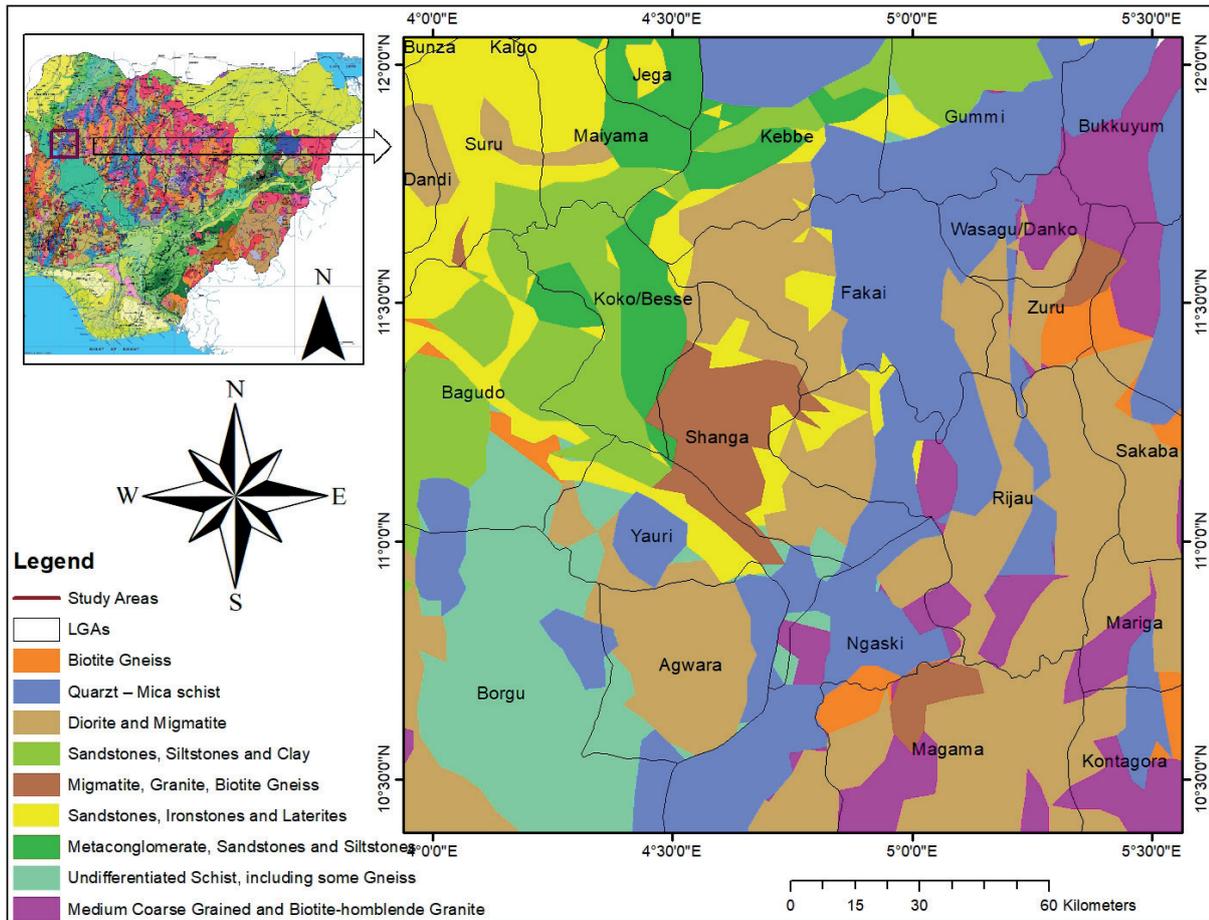
Legend

— Study Areas
☐ LGAs
☐ Biotite Gneiss
☐ Quarzt – Mica schist
☐ Diorite and Migmatite
☐ Sandstones, Siltstones and Clay
☐ Migmatite, Granite, Biotite Gneiss
☐ Sandstones, Ironstones and Laterites
☐ Metaconglomerate, Sandstones and Siltstones
☐ Undifferentiated Schist, including some Gneiss
☐ Medium Coarse Grained and Biotite-homblende Granite

Fig. 1. *Location and geological map of the study area*

METHODOLOGY

Aeromagnetic surveys over parts of the country were carried out by Fugro airborne surveys between 2009 and 2010 on behalf of the Federal Government of Nigeria. The data are under the custody of the Nigeria Geological Survey Agency (NGSA). In this study, nine (9) aeromagnetic datasets were used covering the southern part of Kebbi and the environs of the basement complex of northern Nigeria. These aeromagnetic datasets consist of sheets: 72 Giru, 73 Eokku, 74 Donko, 95 Kaoje, 96 Shanga, 97 Zuru, 117 Konkwesso, 118 Yelwa and 119 Chifu. The data were established under the following high-resolution survey conditions: flight line spacing (500 m), terrain clearance (80 m), tie line spacing (2000 m), flight direction is NW-SE and the tie line direction is NE-SW.

The acquisition of the magnetic dataset involves the attachment of the 3×3 Scintrex CS3 cesium vapour magnetometer sensor to a fixed wing of the aircraft. This method measures the admixture of the earth's core field and the field due to magnetically susceptible rocks in the crust combined with the remanence field of the rocks. The acquired data were corrected by removing the geomagnetic gradient using the main/core field (International Geomagnetic Reference Field IGRF). The data was collected in grid form which was further converted into a digitized form (X, Y and Z). The X and Y represent longitude and latitude respectively measured in meters [m] and Z represent the magnetic intensity measured in nanoteslas [nT].

The acquired dataset was further processed with the aid of the minimum curvature gridding method to produce the total magnetic intensity (TM) map.

DATA PROCESSING

In this study, different processing techniques were employed to process, enhance, and interpret magnetic data with aid of Geosoft (Oasis Montaj) and Surfer software. These techniques include: reduction of magnetic equator (RTE), first vertical derivative (FVD), second vertical derivative (SVD), source parameter imaging (SPI) and analytic signal (AS). The total magnetic field intensity (TMI) value acquired from NGSA which was short-up 33,000 nT for the convenience of contouring or imaging. For these reasons, the value (33,000 nT) must be added back to give the TMI grids for the area (Augie & Ologe 2020, Augie & Ridwan 2021). The generated core fields (DGRF for the epoch period) are subtracted from the grid values (TMI) to give the magnetic anomaly (TMI anomaly).

Reduction to magnetic equator (RTE) technique

The study area falls within magnetic equatorial zones of low inclination (low latitudes) where the reduction to pole technique cannot be applied because the North to South bodies have no detectable induced magnetic anomaly at zero geomagnetic inclination. This technique can make the data easier to interpret without losing any geophysical meaning. At low latitudes, a separate amplitude correction is usually required so as to prevent the North-South signal in the data from dominating the results. As a result, reduced to the pole data may present a less "honest" view of the data (Holden et al. 2008, Core et al. 2009).

RTE techniques usually has an amplitude component $[\sin(I)]$ and a phase component $[i\cos(I)\cos(D - \theta)]$. The values are always synchronized as given below:

$$L(\theta) =$$
$$= \frac{[\sin(I) - i\cos(D-\theta)]^2 \times [-\cos^2(D-\theta)]}{[\sin^2(Ia) + \cos^2(Ia)\cos^2(D-\theta)] \times [\sin^2(I) + \cos^2(D-\theta)]}, \quad (1)$$

$$\text{if } (Ia| < I), \quad Ia = 1$$

where I is geomagnetic inclination [°], D is geomagnetic declination [°] and Ia is inclination for amplitude correction (never less than 1). Equation (1) gives the field strength that is usually required for apparent susceptibility calculation.

Through this equation, the TMI map was reduced to the magnetic equator in order to produce anomalies which depend on the inclination and declination of magnetized body, the local earth's field and orientation of the body with respect to the magnetic north. The resultant composite color depicts reduced-to-equator magnetic anomalies.

First and second vertical derivatives (FVD & SVD) techniques

FVD and SVD filters were applied to the TMI anomaly in order to quantify the spatial rate of change of the magnetic field in horizontal or vertical directions. This derivative enhances high frequency anomalies (that is shallow features) relative to low frequency anomalies (or deep features) and sharpens the edges of anomalies (Adewumi & Salako 2018).

Vertical derivatives are a measure of curvature, and large curvatures are associated with shallow anomalies (Adetona et al. 2018). Thus, it enhances near-surface features at the expense of deeper anomalies. The anomaly in FVD is considerably narrow and more closely reflects the width of the magnetic rock body causing it and the derivatives are given in Equation (2):

$$L(r) = r^n \quad (2)$$

where n – order of differentiation.

SVD is more effective than FVD and it seeks to provide much more detail, emphasizing and enhancing the high frequency parts as observed in the RTE map.

Analytical signal amplitude (ASA) technique

The ASA technique was applied to the RTE grid map to estimate source characteristics and to locate the positions of the causative body. Unlike RTE, this method does not require the direction of the magnetization source prior to the application of the filter. The AS filter is defined as the square root of the sum of the vertical and horizontal derivatives of a magnetic field as defined by Roest et al. (1992) and Pham et al. (2020).

The analytical signal amplitude can now be calculated as:

$$|A(x,y)| = \sqrt{\left(\frac{\partial M}{\partial x}\right)^2 + \left(\frac{\partial M}{\partial y}\right)^2 + \left(\frac{\partial M}{\partial z}\right)^2} \qquad (3)$$

where total magnetic field and *x*, *y* and *z* are the directions and $A(x, y)$ is the amplitude of the analytic signal at (x, y); *M* is the observed magnetic field at (x, y).

Centre for Exploration Targeting (CET) technique

The CET technique was also applied to the RTE grid data anomaly for structural analysis in order to locate the boundaries between sedimentary regions and basement complex areas to help determine the fractures, faults or shears zones, and detect the position of outcrops and intrusive bodies in the area (Adetona et al. 2018).

The procedure gives functionalities to highlight and direct underlying intricacy analysis of aeromagnetic data (Holden et al. 2008, Core et al. 2009). It delineates lineaments with areas of promising mineralization potential via outlining regions of convergence and also the divergence of structural elements using algorithm steps which include: texture analysis, entropy, standard deviation, lineation vectorization, amplitude thresholding, skeletonization and skeleton to vectors.

Source parameter imaging (SPI) technique

The SPI method was applied to the RTE anomaly to differentiate and characterize regions of deep magnetic sources from those of shallow magnetic sources, and it also determines depth to magnetic source (Thompson 1982). The estimate of the depth (*D*) is independent of the magnetic inclination, declination, dip, strike and any remanent magnetization (Odidi et al. 2020). The SPI technique assumes a step type source model (Smith et al. 1998). The following formula holds:

$$D = \frac{1}{k_{max}} \qquad (4)$$

where k_{max} represents the peak value of *k* which is located over the step source:

$$k = \sqrt{\left(\frac{dA}{dx}\right)^2 + \left(\frac{dA}{dy}\right)^2} \qquad (5)$$

where *A* is tilt derivative (TDR) described as below (Smith et al. 1998).

Tilt derivative (TDR) technique

The tilt derivative and its total horizontal derivative are useful for mapping shallow basement structures and mineral exploration targets (Miller & Singh 1994, Thurston & Smith 1997).

The tilt derivative is defined as:

$$\text{TDR} = \tan^{-1}\left(\frac{\text{VDR}}{\text{THDR}}\right) \qquad (6)$$

where VDR and THDR are first vertical and total horizontal derivatives, respectively, of the total magnetic intensity *T*.

$$\text{VDR} = \frac{dT}{dz} \qquad (7)$$

$$\text{THDR} = \sqrt{\left(\frac{dT}{dx}\right)^2 + \left(\frac{dT}{dy}\right)^2} \qquad (8)$$

The total horizontal derivative of the tilt derivative is defined as:

$$\text{HD\_TDR} = \sqrt{\left(\frac{d\text{TDR}}{dx}\right)^2 + \left(\frac{d\text{TDR}}{dy}\right)^2} \qquad (9)$$

where HD_TDR is in units of radians/distance.

RESULTS AND DISCUSSION

In this study, the following processing techniques were employed: RTE, FVD, SVD, CET and AS.

Total magnetic intensity (TMI) and reduction to magnet equator (RTE) results

Figure 2 is the color image of the IGRF corrected total magnetic intensity (TMI). The map gives the vector sum of all components of the magnetic field. It is primarily used in this study to reveal the magnetic characteristic of the various lithological units in the area. The magnetic signatures range from a low magnetic susceptibility of 32,951.0 nT (minimum) along the western region of the study area, to a high magnetic susceptibility of 33,114.0 nT (maximum) in the southern parts of the region.
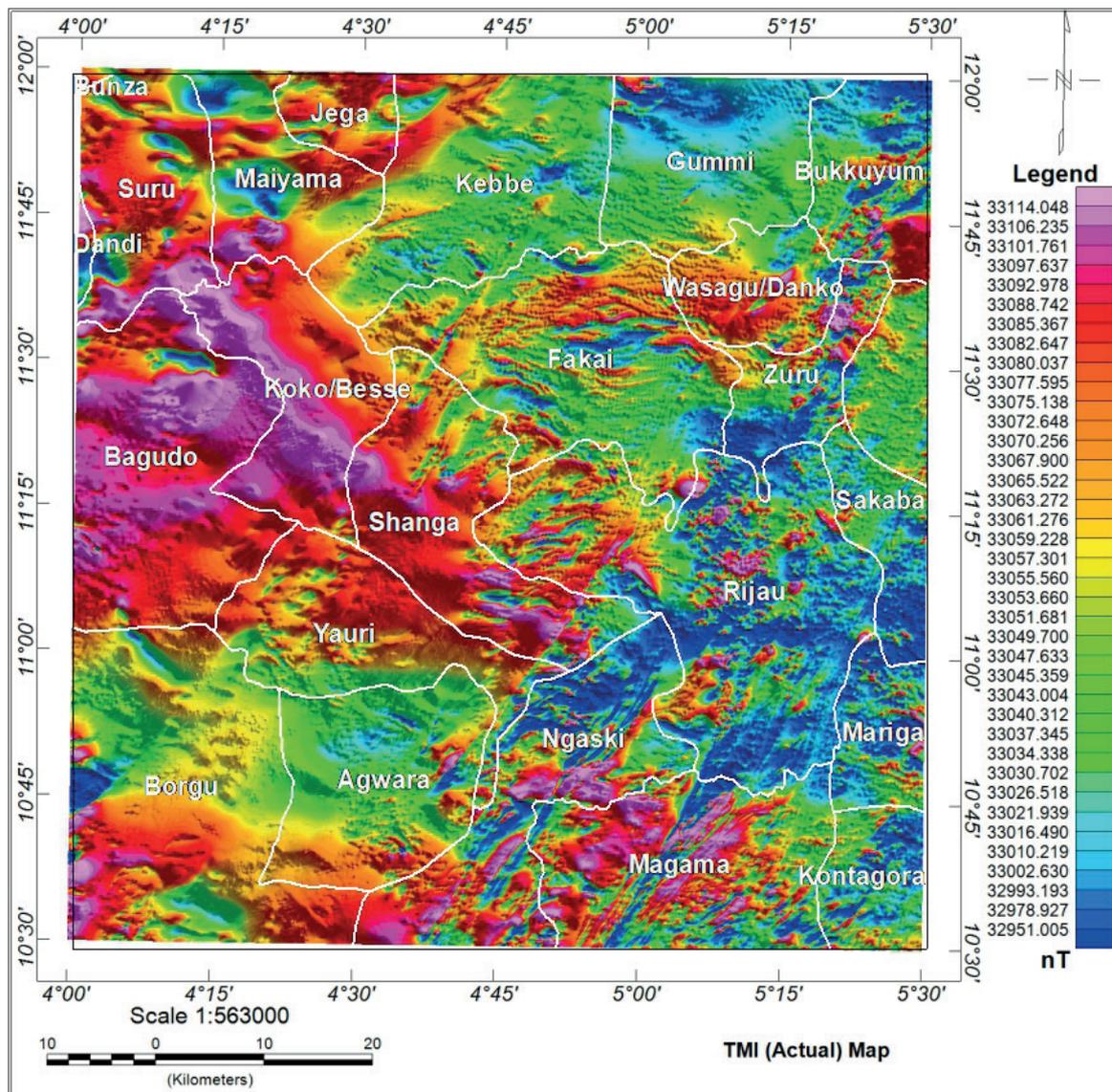
Fig. 2. *Total magnetic intensity (TMI) of the study area*

TMI anomalies were further reduced to the magnetic equator in order to produce anomalies which depend on the inclination and declination of magnetized bodies, the local Earth's field and the orientation of the body with respect to the magnetic north. With the application of reduced to the equator (RTE), the regional magnetic field align horizontally and most of the source magnetizations are horizontal. The resultant composite color depicting reduced-to-equator magnetic anomalies are given in Figure 3. The distinct pattern of highs and lows in Figure 3 and the steep gradients between them at places that describe prominent magnetic lineaments are attributable to the complex assemblage of features with varied dimensions and direction.

The high magnetic trend, marked with a red or pink color, is exhibited by anomalies ranging from 33,074.8 nT to 33,108.7 nT. These regions were corresponded to the following areas; Bagudo, Koko/Besse, Suru, Shanga, the northern part of Zuru, Yauri, the southern part of Ngaski, Wasagu/Danko, the northern part Borgu and Magama. While Areas with low magnetic anomalies, marked in a blue color, ranged from 32,959.0 nT to 33,027.7 nT. These zones corresponded to the

southern part of Zuru, Sakaba, the northern part of Ngaski, Rijau, Mariga and northern parts of Gummi and Bukkuyum. The areas with moderate magnetic trends are: Fakai, Kebbe, the southern part of Gummi, Agwara and the northern part of Borgu (see Fig. 3).

Thus, low and high regions, shown in different color aggregates, are characterized by different rock formations that lead to variations in the magnetic susceptibility of the rocks within the area and usually the susceptible rocks happen at depths shallower than the curie point isotherm.

First vertical derivative (FVD) and second vertical derivative (SVD) results

FVD map (Fig. 4) enhanced the spatial and structural resolution in the area, thereby showing major structural and lithological detail which did not previously appear on the TMI and RTE maps (Figs. 2, 3). Looking at Figure 4 carefully, most of the structures delineated are found within the south-eastern and north-eastern part of the study area. These areas correspond to: SE parts of Yauri and Shanga, Fakai, Ngaski, Zuru, Magama, Rijau, the eastern part of Wasagu/Danko and Bukkuyum.
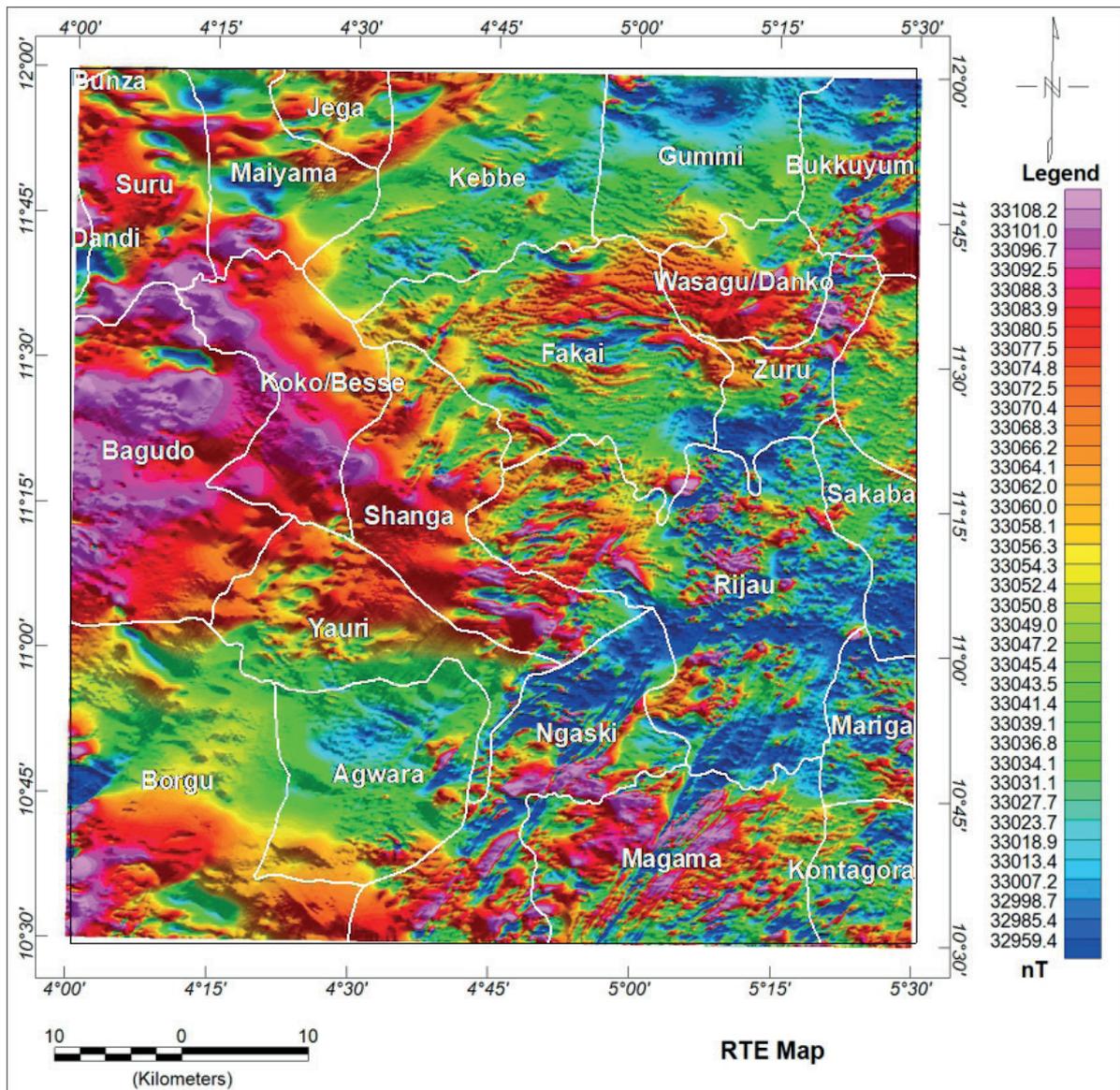

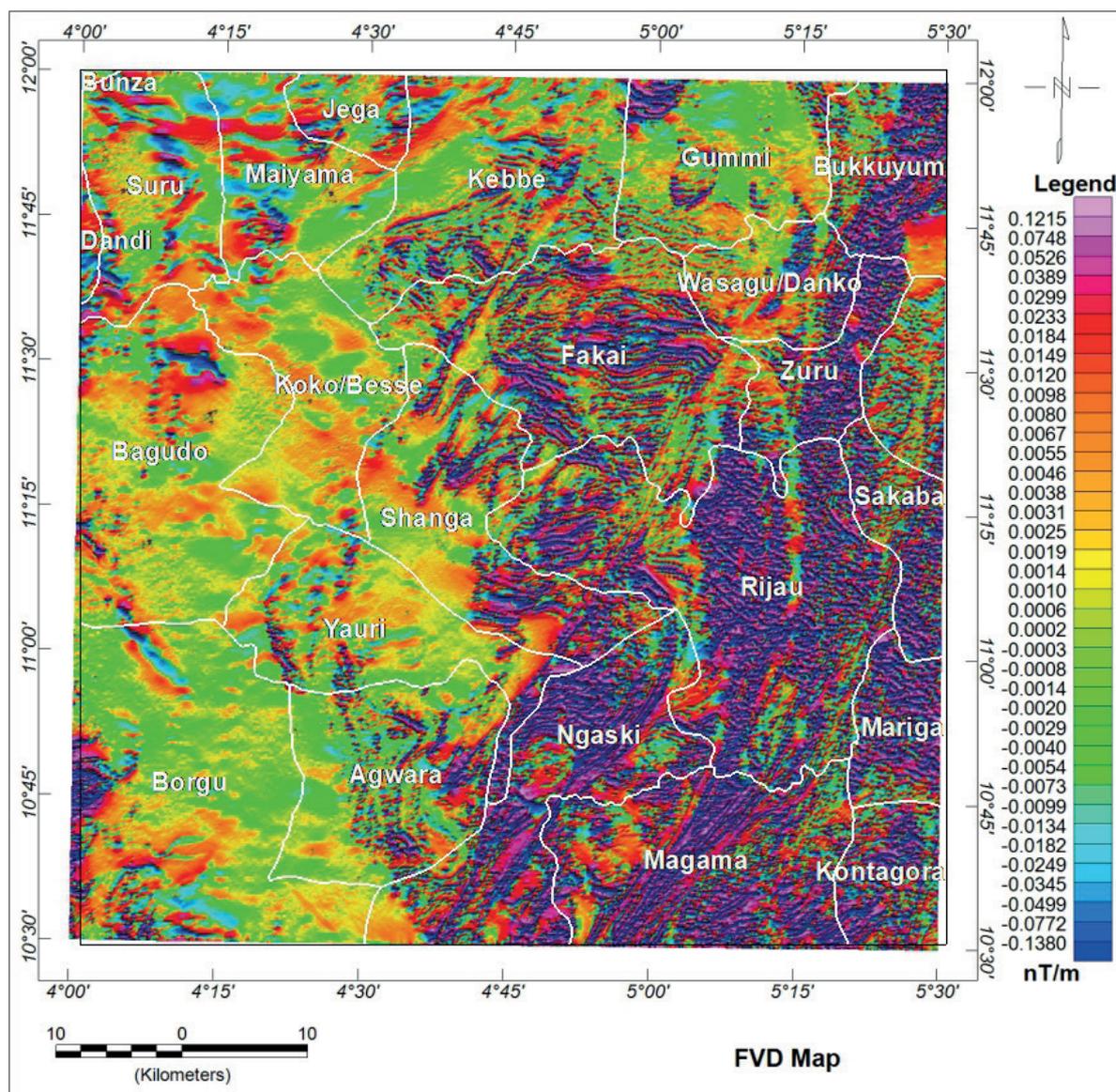***Fig. 3.*** *Reduction to magnetic equator (RTE) map of the study area*

Fig. 4. *First vertical derivative (FVD) map of the study area*

The SVD filter was also applied to RTE anomaly map. The result of SVD map reduces the shallower structures of the causative magnetic rock body, and it enhanced anomaly boundaries of near surface effects that usually characterized the edges of the causative bodies (Fig. 5).

These maps enhanced the major structures/or lineaments such as faults and shear zones which were discovered and trended in NE to SW directions of the study area. The structures found within the aforementioned areas are the architecture of a mineralized body and, according to the geological setting (Fig. 1) of the area, the regions are comprised of the following rock material: quartz-mica schist, granite, biotite, gneiss, diorite, medium coarse-grained and biotite hornblende granite. The magnetic characteristics of the rock formation usually determine the Fe-bearing mineral species present (gold) and the different types of magnetizations displayed by the magnetic mineral species. Most of the structures found in the area correspond to areas of the basement complex as compared with the geological map of the study area (Fig. 1).
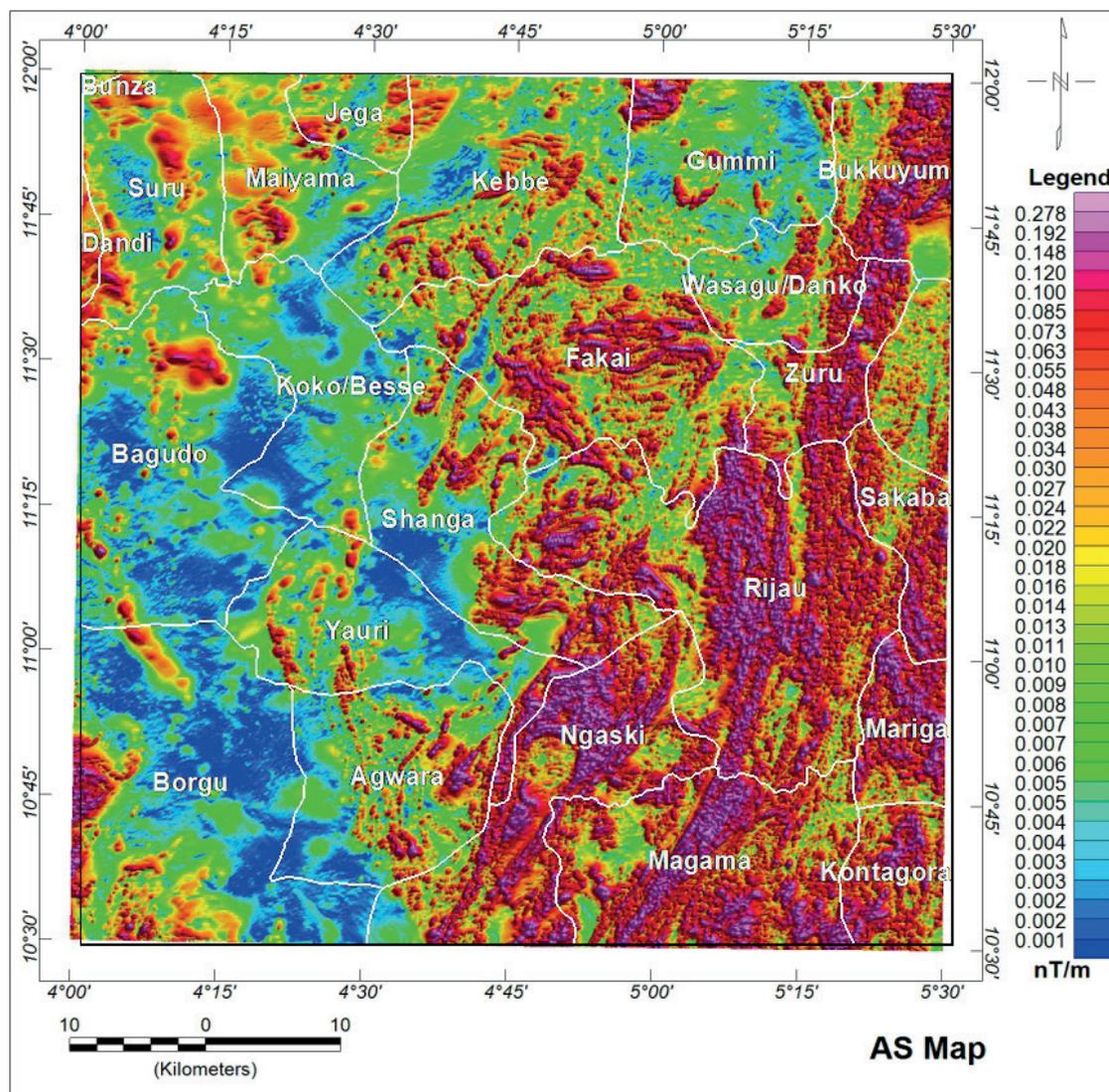
Fig. 5. *Second vertical derivative (SVD) map of the study area*

Analytic signal result

The obtained analytic signal map (Fig. 6) enhanced the variation in the magnetization of the magnetic sources in the area and also indicates the boundaries of anomaly texture. This filter enhances near surface basement. Looking at the map closely, the amplitude is high over the edge of the magnetic structures due to magnetic anomalies around the regions and this could usually be associated with the presence of ferromagnetic, Fe bearing rocks with some felsic minerals as compared with the geological setting of the area and in relation to Figure 7. The map displayed three

different magnetic zones with difference color aggregates. These zones are: low, in a blue color (0.001–0.005 nT/m), moderate, marked with a green-yellow color (0.006–0.043 nT/m) and high, in pink color (above 0.048 nT/m).

Low magnetic zones, shown in blue (Fig. 6), have the low amplitudes ranged from 0.001 nT/m to 0.005 nT/m which were corresponds to: Bagudo, Koko/Besse, Suru, Shanga, the northern part of Zuru, Yauri, the southern part of Ngaski, Wasagu/Danko, the northern part of Borgu and Magama. These zones were associated with sandstones, siltstones, clay shales, limestone and laterites as compared with the geology of the area.

Fig. 6. *Analytical signal (AS) map of the study area*

From Figure 6, it can be seen that the susceptibility values coincided with that of the carbonaceous sedimentary rocks when considered in relation to Figure 7. The sediments within a zone maybe strongly controlled by the carbonate content of the depositional environment and also the carbonates species are usually strongly dependent on both sedimentary facies and sediment provenance.

There are also the zones with a moderate magnetic anomaly, marked in a green or yellow color. These regions have an amplitude ranging from 0.006 nT/m to 0.043 nT/m (Fig. 6) and are associated with meta-conglomerate, mica schist, undifferentiated schist including gneiss, sandstones, ironstones and laterites (Fig. 1). The moderate magnetic anomalous zones correspond to the areas of Fakai, Kebbe, the southern part of Gummi, Agwaru and the northern part of Borgu.

However, the zones with the highest amplitude and marked in pink (above 0.048 nT/m) are associated with; granite, rhyolite, biotite-granite, meta-conglomerate, quartz-mica schist, migmatite and gneiss as compared with the geological setting of the area. These regions also fall under the following areas Shanga, Yauri, Ngaski, Zuru, Fakai, Wasagu/Danko and Sakaba areas of Kebbi State, Kebbe and Bukkuyum areas of Zamfara State and, Rijau, Magama and Mariga areas of Niger State.

When compared with the zones of highest amplitudes (above 0.048 nT/m) in relation to Figure 7, it can be observed that the regions exhibit substantial positive magnetic susceptibility values that corresponded to the presence ferromagnetic minerals such as gold. These areas with ferromagnetic properties may usually contain mafic and ultramafic that host more Fe-bearing minerals (gold mineral) as compared in relation to Figure 7. The type of rock formations highlighted in these areas as compared with Figure 7 may contribute significantly to identifying the species of crystallized gold with the increase of the oxidized Fe-bearing minerals from mafic to felsic rocks.

Centre for Exploration Targeting (CET) result

CET map (Fig. 8) reveals the linear structures (lineament) within the south-eastern part of the study area which corresponds to: SE parts of Yauri and Shanga, Fakai, Ngaski, Zuru, Magama, Rijau, the eastern part of Wasagu/Danko and Bukkuyum. These structures were located within the basement regions in the area and correlated well with the geology of the area. From Figure 7, it can be observed that most of the linear structures trending in the NE-SW directions delineate faults, fractures or shears zones that represent vein of mineralization.
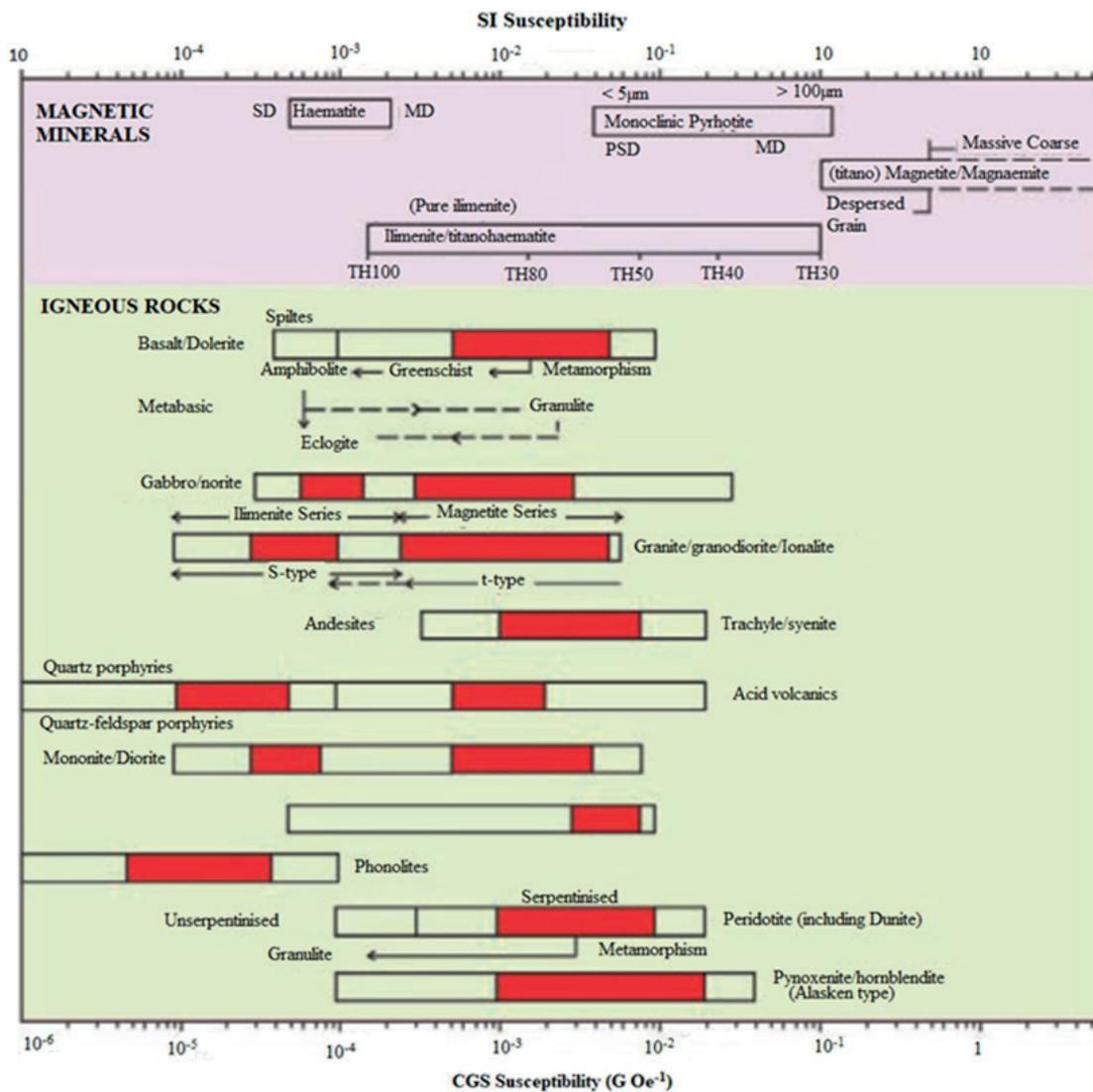

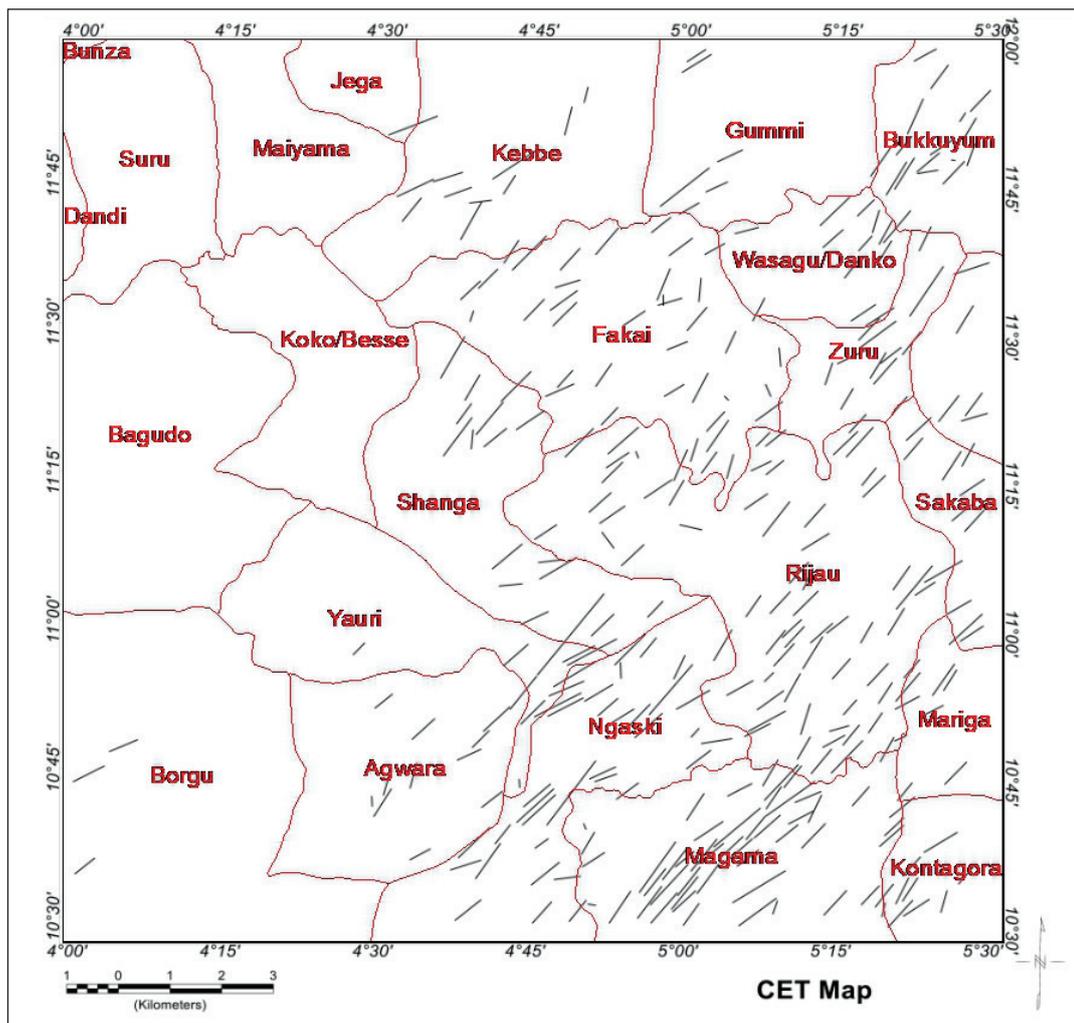**Fig. 7.** *Common magnetic susceptibility ranges for various rock types (Clark 2010)*

Fig. 8. *Centre for Exploration Targeting (CET) map of the study area*

From the geological setting of the area (Fig. 1), the regions fall under the following rock types; quartz-mica schist, migmatite, granite, biotite, gneiss and diorite. These rock types, found within structural trend of alteration zones, play an important role in determining gold mineralization since most gold deposits in Nigeria are found in quartz veins. The CET (Fig. 8) result agreed with the structures/or lineaments found in Figures 3 and 4. The Fe-bearing silicate minerals that form in igneous rocks are commonly includes: olivine, pyroxene, amphibole and mica group, and they are not ferromagnetic (Olugbenga & Augie 2020). Thus, the Fe oxide minerals commonly found in igneous rocks form three significant solid-solution series which are: titanomagnetite with end members magnetite and titanohematite with end members hematite.

The magnetite also explained from geological setting of the study area and the magnetic susceptibility values of some common rocks, as shown in Figure 7, led to the identification of magnetic minerals such as gold within the aforementioned area.

Source parameter imaging (SPI) result

Figure 8 revealed the depth to magnetic sources and also the depth at which basement rock contact, fractures or faults with dykes could be found. Looking at map (Fig. 9) carefully, the depths were categorized into three kind: below 137 m, identified with a pink color, from 150 m to 177 m, with a yellow or green color, above 363 m, with a blue color. The obtained SPI depth map helped in specifying the depth of the boundaries of causative bodies and trends of structures revealed in Figure 7.
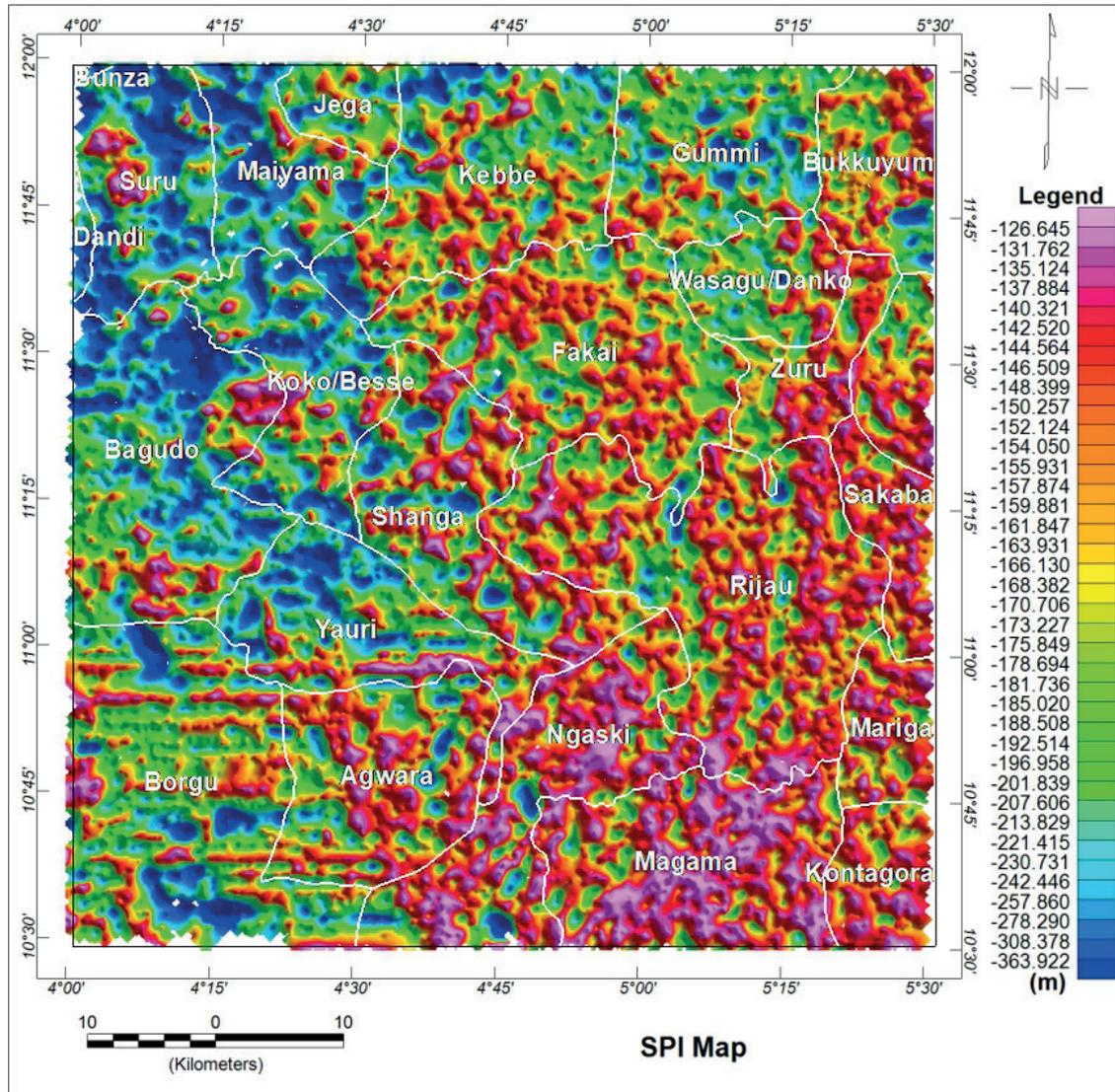
Fig. 9. *Source parameter imaging (SPI) map of the study area*

The zones below 137 m depth, identified with a pink color, correspond to the regions of faults/structural trends identified in the SE parts of Yauri and Shanga, Fakai, Ngaski, Zuru, Magama, Rijau, the eastern part of Wasagu/Danko and Bukkuyum.

Tilt derivative (TDR) result

Figure 10 represents the TDR map of the area that was generated from RTE anomalies of magnetic data. Observing the map closely, it indicates the horizontal location and extent of edges of various magnetic sources that formed lineaments. The edges of the shallow and deep sources were more

pronounced as compared with AS, FVD and SVD Maps. The major structures were found within the south-eastern and north-eastern parts of the area. These areas correspond to: SE parts of Yauri and Shanga, Fakai, Ngaski, Zuru, Magama, Rijau, the eastern part of Wasagu/Danko and Bukkuyum. The structures delineated within these areas revealed the spatial location of the magnetic source edges. These structures could play a role in determining the presence of gold mineral compared with the geological setting of the area. These regions were underlain by granite, rhyolite, biotite-granite, meta-conglomerate, quartz-mica schist, migmatite and gneiss (Fig. 1).
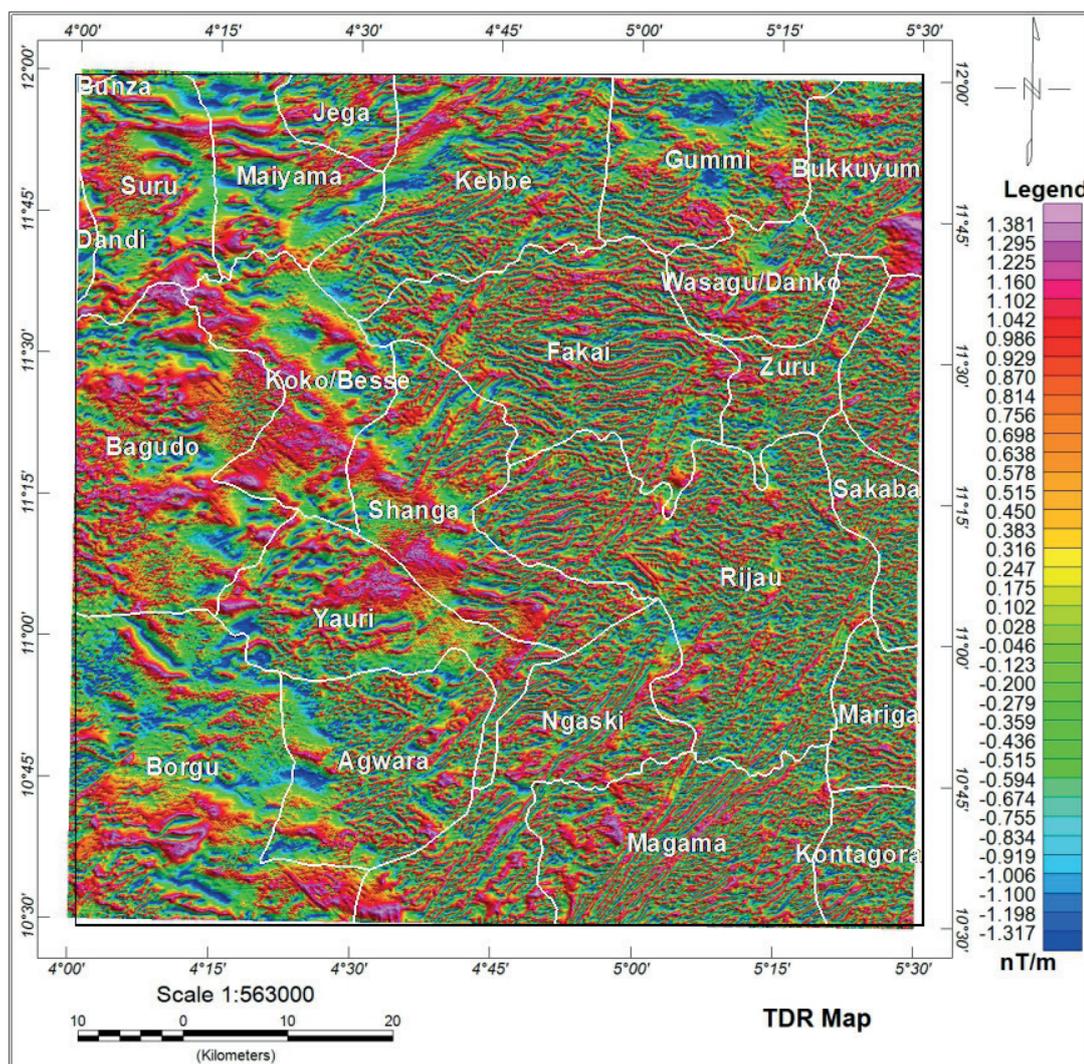
Fig. 10. *Tilt derivative (TDR) map of the study area*

CONCLUSION

The results presented in this study, using the RTE, FVD, SVD, AS, CET, SPI and TDR techniques, have revealed the regions that may host gold mineral. These regions corresponded to the following areas: SE parts of Yauri and Shanga, Fakai, Ngaski, Zuru, Magama, Rijau, the eastern part of Wasagu/Danko and Bukkuyum. These areas fall under the basement complex of northern Nigeria, mainly in the southern part of Kebbi state. The RTE technique has helped in correcting an anomaly in the data, as well as preventing the unwanted NS signal from dominating the results because the area falls within magnetic equatorial zones

of low inclination (low latitudes). This technique was not previously applied to the aeromagnetic studies conducted in the area by the authors: Bonde et al. (2019), Lawali et al. (2020) and Lawal et al. (2021). FVD, SVD, CET and TDR maps enhanced the major structures/or lineaments trending in the NE to SW directions. The map obtained from the application of the analytical signal filter enhanced the variation in the magnetization of the magnetic sources in the area. This map displayed three different magnetic zones in which the amplitudes ranged from 0.001 nT/m to 0.005 nT/m (low amplitude) with a blue color, from 0.006 nT/m to 0.043 nT/m (moderate amplitude) with a green-yellow color, and above 0.048 nT/m

(higher amplitude) with a pink color. The depth to magnetic sources were categorized as: below 137 m (shallower depth) with a pink color, from 150 m to 177 m with a green/yellow color, above 364 m with a blue color (deeper depth) respectively. The zones below 137 m depth correspond to the regions of faults/structural trends identified in aforementioned areas state the area. Most of the linear structures delineated in the area represent veins of mineralization which play an important role in determining the gold mineralization.

REFERENCES

Adetona A.A., Salako K.A. & Rafiu A.A., 2018. Delineating the lineaments within the major structures around eastern part of lower Benue Trough from 2009 aeromagnetic data. *FUW Trends in Science and Technology Journal*, 3, 1, 175–179.

Adewumi T. & Salako K.A., 2018. Delineation of mineral potential zone using high resolution aeromagnetic data over part of Nasarawa State, North Central, Nigeria. *Egyptian Journal of Petroleum*, 27, 4, 759–767. https://doi.org/10.1016/j.ejpe.2017.11.002.

Augie A.I. & Sani A.A., 2020. Interpretation of aeromagnetic data for gold mineralisation potential over Kabo and its environs NW Nigeria. *Savanna Journal of Basic and Applied Sciences*, 2, 2, 116–123.

Augie A.I., Saleh M. & Gado A.A., 2020. Geophysical investigation of abnormal seepages in Goronyo Dam Sokoto, North Western Nigeria using self-potential method. *International Journal of Geotechnical and Geotechnical and Geological Engineering*, 14, 3, 104–107.

Augie A.I., Adamu A., Salako K.A., Alkali A., Narimi A.M., Yahaya M.N. & Sani A.A., 2021a. Assessment for gold mineralisation potential over Anka Schist Belts NW Nigeria Using Aeromagnetic Data. *FUDMA Journal of Sciences (FJS)*, 5, 4, 235–242. https://doi.org/10.33003/fjs-2021-0504-810.

Augie A.I., Salako K.A., Rafiu A.A. & Jimoh M.O., 2021b. Estimation of depth to structures associated with gold mineralisation potential over southern part of Kebbi State using aeromagnetic data. [in:] *3rd School of Physical Sciences Biennial International Conference Futminna 2021*, Federal University of Technology Minna, 290–297.

Augie A.I., Bawa Y.I., Saleh A., Magawata U.Z. & Garba N., 2022. Tracing the structures associated with manganese over western part of Kebbi using aeromagnetic data. *Science Forum (Journal of Pure and Applied Sciences)*, 22, 1, 28–34. https://doi.org/10.5455/sf.augie22.

Bonde D.S., Lawali S. & Salako K.A., 2019. Structural mapping of solid mineral potential zones over southern part of Kebbi State, Northwestern Nigeria. *Journal of Scientific and Engineering Research*, 6, 7, 229–240.

Clark D.A., 2010. Magnetic petrophysics and magnetic petrology: aids to geologic interpretation of magnetic surveys. *AGSO Journal of Austrian Geology and Geophysics*, 36, 2, 83–103.

Cordell L. & Grauch V.J.S., 1985. Mapping basement magnetization zones from aeromagnetic data in the San Juan Basin, New Mexico. [in:] Hinze W.J. (ed.), *The Utility of Regional Gravity and Magnetic Maps*, Society of Exploration Geophysicists, Tulsa, 181–197. https://doi.org/10.1190/1.0931830346.ch16.

Core D., Buckingham A. & Belfield S., 2009. Detailed structural analysis of magnetic data-done quickly and objectively. *SGEG Newsletter*, 1–2, 15–21.

Danbatta U.A., 2005. Precambrian crustal development of the northwestern part of Zuru schist belt, NW Nigeria. *41st Annual Conference of Nigerian Mining and Geosciences Society (NMGS), Nigeria* [paper presented at the conference].

Danbatta U.A., 2008. Precambrian crustal development in the northwestern part of Zuru schist belt, northwestern Nigeria. *Journal of Mining and Geology*, 44, 1, 43–56. https://doi.org/10.4314/jmg.v44i1.18883.

Danbatta U.A., Abubakar Y.I. & Ibrahim A.A., 2008. Geochemistry of gold deposits in Anka schist belt, northwestern Nigeria. *Nigerian Journal of Chemical Research*, 13, 19–29.

Danjumma S.G., Bonde D.S., Mohammed A., Lawali S. & Amina M.B.T., 2019. Identification of mineral deposits in Garin Awwal Mining Site, Kebbi State, northwestern Nigeria. *Journal of Multidisciplinary Engineering Science and Technology (JMEST)*, 6, 6, 10276–10280.

Ejepu J.S., Unuevho C.I., Ako T.A. & Abdullahi S., 2018. Integrated geosciences prospecting for gold mineralization in Kwakuti, North-Central Nigeria. *Journal of Geology and Mining*, 10, 7, 81–94. https://doi.org/10.5897/JGMR2018.0296.

Evjen H.M., 1936. The place of the vertical gradient in gravitational interpretations. *Geophysics*, 1, 1, 127–136. https://doi.org/10.1190/1.1437067.

Fedi M. & Florio G., 2001. Detection of potential fields source boundaries by enhanced horizontal derivative method. *Geophysics Prospect*, 49, 1, 40–58. https://doi.org/10.1046/j.1365-2478.2001.00235.x.

Holden E.J., Dentith M. & Kavesi P., 2008. Towards the automatic analysis of regional aeromagnetic data to identify regions prospective for gold deposits. *Computer Geoscience*, 34, 1505–1513. https://doi.org/10.1016/j.cageo.2007.08.007.

Kearey P., Brooks M. & Hill I., 2002. *An Introduction to Geophysical Exploration*. Blackwell Scientific Publications, New York.

Lawal M.M., Salako K.A., Abbas M., Adewumi T., Augie A.I. & Khita M., 2021. Geophysical investigation of possible gold mineralization potential zones using a combined airborne magnetic data of lower Sokoto Basin and its environs, northwestern Nigeria. *International Journal of Progressive Sciences and Technologies (IJPSAT)*, 30, 1, 1–16.

Lawali S., Salako K.A. & Bonde D.S., 2020. Delineation of mineral potential zones over lower part of Sokoto Basin, northwestern Nigeria using aeromagnetic data. *Academic Research International*, 11, 2, 19–29.

Miller H.G. & Singh V.J. 1994. Potential field tilt: a new concept for location of potential field sources. *Applied Geophysics*, 32, 213–217. https://doi.org/10.1016/0926-9851(94)90022-1.

Odidi I.G., Mallam A. & Nasir N., 2020. Depth to magnetic sources determination using Source Parameter Imaging (SPI) of aeromagnetic data of parts of Central and North-Eastern Nigeria: A reconnaissance tool for geothermal exploration in the area. *Science World Journal*, 15, 3, 19–23.

Olalekan O., Afees O. & Ayodele S., 2016. An empirical analysis of the contribution of mining sector to economic development in Nigeria. *Journal of Humanities and Social Sciences*, 19, 1, 88–106. https://doi.org/10.5782/2223-2621.2016.19.1.88.

Olugbenga T.T. & Augie A.I., 2020. Estimation of crustal thickness within the Sokoto Basin, North-Western Nigeria using bouguer gravity anomaly data. *International Journal of Geological and Environmental Engineering*, 14, 9, 247–252.

Pham L.T., 2021. A high resolution edge detector for interpreting potential field data: A case study from the Witwatersrand Basin, South Africa. *Journal of African Earth Sciences*, 178, 104190. https://doi.org/10.1016/j.jafrearsci.2021.104190.

Pham L.T., Oksum E., Do T.D., Le-Huy M., Vu M.D. & Nguyen V.D., 2019. LAS: A combination of the analytic signal amplitude and the generalised logistic function as a novel edge enhancement of magnetic data. *Contributions to Geophysics and Geodesy*, 49, 4, 425–440. https://doi.org/10.2478/congeo-2019-0022.

Pham L.T., Vu T.V., Thi S.L. & Trinh P.T., 2020. Enhancement of potential field source boundaries using an improved logistic filter. *Pure and Applied Geophysics*, 177, 5237–5249. https://doi.org/10.1007/s00024-020-02542-9.

Pham L.T., Oksum E., Le D.V., Ferreira F.J.F. & Le S.T., 2021. Edge detection of potential field sources using the softsign function. *Geocarto International*. https://doi.org/10.1080/10106049.2021.1882007.

Pham L.T., Eldosouky A.M., Oksum E. & Saada S.A., 2022. A new high resolution filter for source edge detection of potential field data. *Geocarto International*. 37, 11, 3051–3068. https://doi.org/10.1080/10106049.2020.1849414.

Ramadan T.M. & AbdelFattah M.F., 2010. Characterization of gold mineralization in Garin Hawal area, Kebbi State, NW Nigeria, using remote sensing. *Egyptian Journal of Remote Sensing and Space Science*, 13, 2, 153–163. https://doi.org/10.1016/j.ejrs.2009.08.001.

Reeves C., 2005. *Aeromagnetic Surveys: Principles, Practice and Interpretation*. Earthworks-Global Thinking in Exploration Geoscience, Geosoft.

Roest W.R., Verhoef J. & Pilkington M., 1992. Magnetic interpretation using 3-D analytic signal. *Geophysics*, 57, 1, 116–125. https://doi.org/10.1190/1.1443174.

Sani A.A., Augie A.I. & Aku M.O., 2019. Analysis of gold mineral potentials in Anka schist belt, north western Nigeria using aeromagnetic data interpretation. *Egyptian Journal of Remote Sensing and Space Science*, 52, 291–298.

Sani M.A., Raimi J., Elatikpo S.M. & Lawal K.M., 2017. Magnetic interpretation of structures associated with gold mineralisation around Kundila and Ginzo area, northwestern Nigeria. *Nigerian Journal of Scientific Research*, 16, 2, 240–246.

Smith R.S., Thurston J.B., Dai T.F. & MacLeod I.N., 1998. iSPI™ the improved source parameter imaging method. *Geophysical Prospecting*, 46, 2, 141–151. https://doi.org/10.1046/j.1365-2478.1998.00084.x.

Tawey M.D., Alhassan D.U., Adetona A.A., Salako K.A., Rafiu A.A. & Udensi E.E., 2020. Application of aeromagnetic data to assess the structures and solid mineral potentials in part of North Central Nigeria. *Journal of Geography, Environment and Earth Science International*, 24, 5, 11–29. https://doi.org/10.9734/jgeesi/2020/v24i530223.

Thompson D.T., 1982. EULDPH: A new technique for making computer-assisted depth estimates from magnetic data. *Geophysics*, 47, 1, 31–37. https://doi.org/10.1190/1.1441278.

Thurston J.B. & Smith R.S., 1997. Automatic conversion of magnetic data to depth, dip and susceptibility contrast using the SPITM method. *Geophysics*, 62, 3, 807–813. https://doi.org/10.1190/1.1444190.